EasyChair Preprint

№ 11992

Structural, Mechanical, and Electronic Properties of the Oxide Perovskite XNpO3 (X=Eu and Gd): a DFT Study

Youssef Didi, Soufiane Bahhar, Abdelilah Rjeb, Abdellah Tahiri and Mohamed Naji

February 9, 2024

Structural, mechanical, and electronic properties of the oxide perovskite $XNpO_3$ (X=Eu and Gd): A DFT study

Youssef Didi[1], Soufiane Bahhar[2], Abdelilah Rjeb[1], Abdellah Tahiri[1], Mohamed Naji[1].

[1]LPAIS, Faculty of Sciences, Sidi Mohamed Ben Abdellah University, B.P. 1796 Fez -Atlas, Morocco
[2]Faculty of Sciences, Department of Physics, Chouaïb Doukkali University, El-Jadida, Morocco

Abstract

This study describes the discovery of two new perovskite-type oxides ($XNpO_3$: X=Eu and Gd) using computational methods like density functional theory (DFT) in the CASTEP code. It delves into their structural, electronic, mechanical, and optical properties, revealing their half-metallic nature through band structures (BS) and density of states diagrams. The materials exhibit mechanical stability in line with Born's criteria, demonstrated by their elastic constants. Additionally, their properties suggest potential uses in optoelectronic devices for capturing ultraviolet light and applications in thermoelectric and spintronic devices.

1. Introduction

The perovskite, a material widely employed in the fields of microelectronics, electrochemistry, and optoelectronics due to its diverse properties such as ionic conduction, catalysis, dielectric, and ferroelectricity [1-4], also garners interest as a potential candidate for immobilizing highly radioactive nuclear waste, including actinides and certain long-lived fission products [5,6]. However, radiation from the alpha decay of actinides and the beta decay of fission products causes cumulative damage in perovskites, leading to structural alterations and deterioration of their physical and chemical durability. Therefore, understanding and predicting the behavior of perovskites in irradiated environments is crucial, both for assessing their performance and for designing advanced materials. Perovskites ABO_3 based on actinides have been studied using density functional theory (DFT) [7,8]. Most of these perovskites exhibit a semi-metallic nature due to localized f states. For instance, Zahid et al. investigated $BaXO_3$ perovskites (X =Pr, U) and observed the persistence of the semi-metallic nature in these

compounds [9]. In a similar context, the works of Shakeel et al. [10] and M. Nabi et al. [11] focused on actinide-based ceramics BaXO3. Their studies revealed that $BaNpO_3$ and $BaBkO_3$ materials exhibit a semi-metallic nature, holding promising prospects for spintronics and thermoelectricity. Additionally, Sakshi et al. predicted that $SrMO_3$ is thermodynamically stable and semi-metallic [12]. Among these perovskite materials, $EuNpO_3$ and $GdNpO_3$ belong to a family of perovskite oxides that contain both rare earth elements (Eu or Gd) and actinides (Np) [13]. These compounds exhibit a fascinating combination of features, including semi-metallicity and strong magnetic interactions, making them highly attractive for various technological applications. The presence of the actinide element, neptunium (Np), in these perovskite structures further adds to their uniqueness. Np is a radioactive element with interesting nuclear properties [14], and its confinement within a solid matrix can have significant implications for both fundamental research and practical applications. The confinement of nuclear neptunium in $EuNpO_3$ and $GdNpO_3$ not only provides a means to study the behavior of actinide elements at the atomic level but also offers potential avenues for the safe storage and disposal of radioactive waste [15].

The objective of this study is to analyze the structural, electronic, and magnetic properties of $EuNpO_3$ and $GdNpO_3$ compounds using density functional theory (DFT) simulations, with a particular emphasis on the nuclear confinement of neptunium. By understanding the interaction between electronic structure, magnetic order, and nuclear confinement, valuable insights can be gained into the behavior of actinide-based perovskites, thereby opening new possibilities for their application in fields such as spintronics, catalysis, and nuclear waste management.

2. Computational details

In the current research, the CASTEP code [16] was employed to conduct our DFT study. All calculations were performed on single-cell units using the Vanderbilt ultrasoft pseudopotential (USPP) approach. The exchange-correlation potential was computed using the Perdew Burke Ernzerhof approximation and the generalized gradient approximation (PBE GGA) [17]. Geometry optimization of Neptunium-based perovskite-type oxides $XNpO_3$ (X = Eu and Gd) was carried out, implementing periodic boundary conditions extended by a planewave basis set through the Bloch theorem [18]. The calculations involved the explicit treatment of specific valence states: Eu ($4f^7\ 5s^2\ 5p^6\ 6s^2$), Gd ($4f^7\ 5s^2\ 5p^6\ 5d^1\ 6s^2$), Np ($5f^4\ 6s^2\ 6p^6\ 6d^17s^2$), and O ($2s^2\ 2p^4$). The Monkhorst Pack scheme was utilized in the first Brillouin zone. To ensure reliable results, an ultra-fine k-point mesh ($8 \times 8 \times 8$) was selected, and the energy cutoff value was set to 600 eV, with a smearing value of 0.1 eV. In terms of energy, the maximum ionic force per atom was 0.01 eV/Å, and the energy convergence was set at 5×10^{-6} eV/atom. The maximum displacement was 5×10^{-4} Å, and the maximum pressure was 0.02 GPa. In the context of crystalline materials, electronic wave functions and charge densities were calculated using the Broyden, Fletcher, Goldfarb & Shanno energy minimization method (BFGS) [19], a preferred and widely used algorithm in the literature. This primary algorithm was employed to optimize all structures for the calculation of structural and electronic properties. Finally, it should be noted that all DFT calculations were conducted at 0 K and 0 GPa.

3. Structural properties

The crystalline structure of neptunium-based perovskite oxides $XNpO_3$ (X = Eu, Gd) is depicted in Fig.1. The two optimized $ANpO_3$ oxides (X = Eu, Gd) crystallize in a simple cubic structure (fcc) with space group Pm-3m number 221, in accordance with international table specifications. In this crystalline structure, atoms of X (Eu, Gd) occupy the corners of the unit cell 1a (0, 0, 0), Np atoms are positioned at the center 1b (0.5, 0.5, 0.5), and oxygen atoms (O) are located at the center of the faces of the ABO_3 unit cell, i.e., at atomic coordinates 3c (0, 0.5, 0.5), 3c (0.5, 0, 0.5), and 3c (0.5, 0.5, 0). This atomic arrangement provides a coordination of 9 neighbors for the three X cations (Eu, Gd) and a coordination of 6 neighbors for the Np cation. The table compiles the optimized lattice parameters, volume, and density of the $XNpO_3$ compounds. As shown in Table 1, $EuNpO_3$ has the largest lattice parameter with a value of 4.407 Å, while $GdNpO_3$ has a relatively smaller lattice parameter (a = 4.396 Å). Regarding density (ρ), $GdNpO_3$ exhibits the highest density (ρ = 8.640 g/cm3) compared to $EuNpO_3$ (ρ = 8.471 g/cm3). To the authors' knowledge, perovskites $XNpO_3$ (X = Eu, Gd) have never been studied. Thus, this research is expected to make a significant and valuable contribution to the future exploration of $XNpO_3$ oxides (X = Eu, Gd).

Table 1

The optimized lattice parameter a, volume V and density ρ for XNpO3.

Compound	a (Å)	V (Å^3)	ρ (g/cm^3)
$EuNpO_3$	4.407	85.622	8.471
$GdNpO_3$	4.396	84.994	8.640

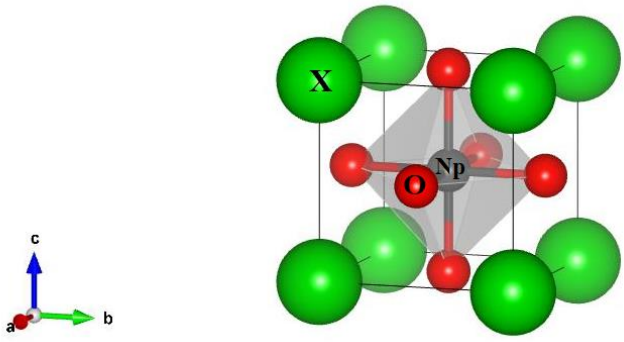

Fig1: optimized cubic crystal structure of $XNpO_3$ (X = Eu, Gd).

4. Electronic properties

Perovskite oxides are attractive materials for various applications, where their electronic properties are still being explored and understood. In this subsection, we delve into the electronic characteristics of $XNpO_3$ perovskites (X = Eu, Gd), with a particular focus on their band structure (BS), total density of states (DOS), and partial density of states (PDOS), which are calculated and discussed in this section. Two types of electronic bands exist as they provide details on electron accessibility. One is called the conduction band (CB), which appears beyond the Fermi level (EF), while the other is called the valence band (VB), located below the EF.

The band gap can be obtained by calculating the difference between the minimum value of the CB and the maximum value of the VB. The electronic band can be explained as direct or indirect. The direct band refers to a band in which the minima of the CB (CBM) and the maxima of the VB (VBM) are located at the same point. However, the presence of CBM and VBM at separate locations leads to the establishment of an indirect band to represent the BS. Fig.2 depicts the electronic band structure of $XNpO_3$ phases, where the solid horizontal line in black represents the Fermi level (Ef). The calculated band structures follow the standard k path X → R → M → G → R for a cubic $Pm\bar{3}m$ structure. The band structure curves near the Fermi level are an extremely informative guide to the material's nature, whether it is half-metallic, as these materials exhibit metallic character in an up-spin channel, and in contrast to the down-spin, reveal semiconductor behavior

The density of states (DOS) is employed to elucidate the electrical and optical properties of a system. The total density of states (TDOS) and partial density of states (PDOS) are calculated for the optimized lattice parameter based on geometric optimization. The plots of TDOS also confirm that all components are semiconductors. The total DOS, crucial for both $EuNpO_3$ and $GdNpO_3$ materials, is presented in Fig.3. They are calculated based on the eigenvalues and eigenvectors obtained at the appropriate k-points (21x21x21).

5. Mechanical properties

The distinct mechanical behavior of perovskite-type materials can be studied using elastic constants. These parameters provide a precise measurement of a material's response to mechanical stress, while also offering crucial insights into its stiffness, deformability, and ability to withstand deformation under external stresses. Elastic constants for cubic structures can be characterized by three independent

variables (Cij), typically denoted as C_{11}, C_{12}, and C_{44}. Table 2 summarizes the theoretical elastic constants calculated for $EuNpO_3$ and $GdNpO_3$.

Mechanical stability indications can be obtained from these elastic constants. Mechanical stability criteria include the requirement that the eigenvalues of the calculated elastic constants matrix be positive. The conditions set for cubic symmetry state that: $C_{11} > 0$, $C_{12} > 0$, $C_{44} > 0$, and C_{11}-$C_{12} > 0$ [20]

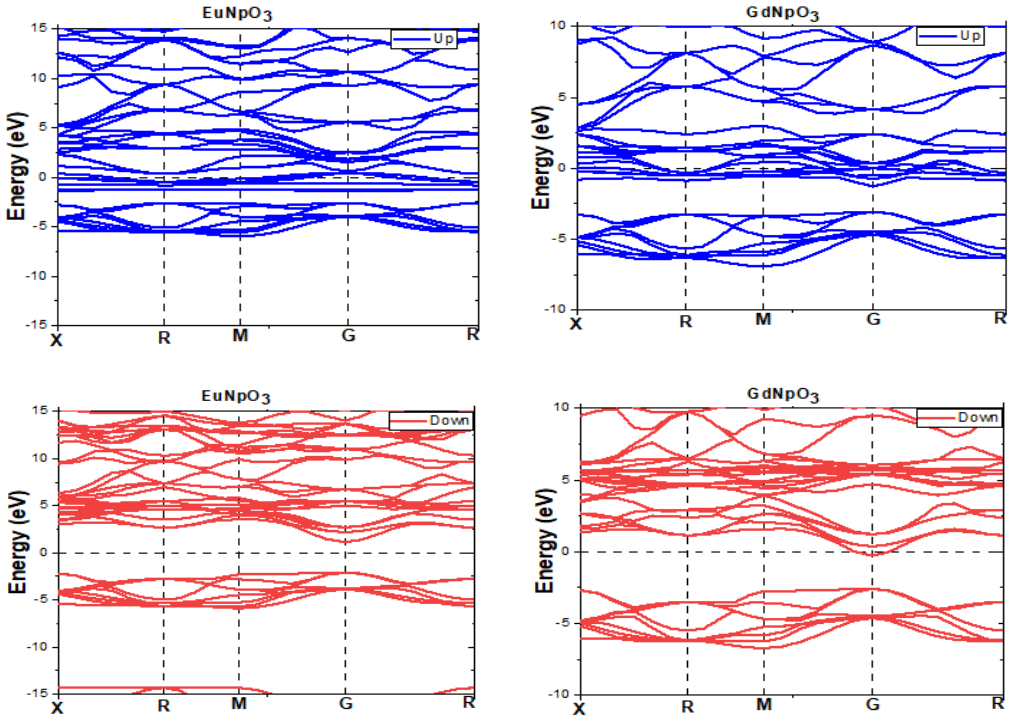

Fig 2: Band structures of $EuNpO_3$ and $GdNpO_3$

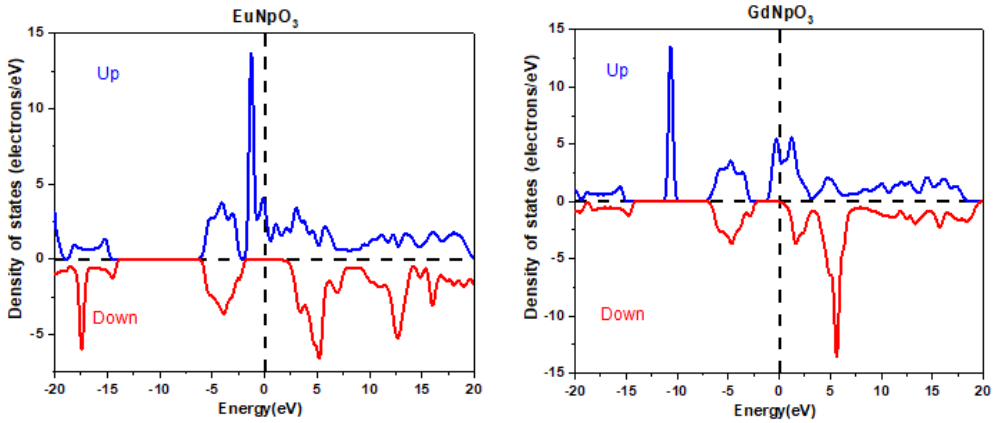

Fig3: Total density of the components, $EuNpO_3$ and $GdNpO_3$.

Table 2

Elastic constants C_{ij} (GPa) and calculated Cauchy pressure C_{12}-C_{44} (GPa) for $XNpO_3$ perovskites

Compound	C_{11} (GPa)	C_{12} (GPa)	C_{44} (GPa)	$C_{12}-C_{44}$ (GPa)
$EuNpO_3$	213.58840	74.86170	40.86095	172.727
$GdNpO_3$	207.54595	77.1320	10.5265	197.0194

Conclusion

The mechanical, electrical, structural, and optical properties of the material were examined using the pseudo-potential plane wave (PP-PW) method based on density functional theory, as well as the general gradient approximation GGA. The results are summarized below: The analysis of the band structure and density of states (DOS) highlighted a semi-metallic behavior in both materials. Additionally, the oxides $XNpO_3$ (X = Eu, Gd) demonstrated mechanical stability in accordance with Born's stability criteria. The latter shows significant potential for optoelectronic devices capturing ultraviolet light from solar radiation.

References

[1] M. Kajitani, M. Matsuda, A. Hoshikawa, S. Harjo, T. Kamiyama, T. Ishigaki, F. Izumi, M. Miyake, In situ neutron diffraction study on fast oxide ion conductor LaGaO3-based perovskite compounds, Chem. Mater. 17 (2005) 4235–4243, https://doi.org/10.1021/cm050597n.

[2] M.V. Kovalenko, L. Protesescu, M.I. Bodnarchuk, Protesescu Loredana, Properties and potential optoelectronic applications of lead halide perovskite nanocrystals, Science. 358 (6364) (2017) 745–750.

[3] C.C. Hu, Y.L. Lee, H. Teng, Efficient water splitting over Na1-xKxTaO3 photocatalysts with cubic perovskite structure, J. Mater. Chem. 21 (2011) 3824–3830, https://doi.org/10.1039/c0jm03451g.

[4] H. Salehi, First principles studies on the electronic structure and band structure of paraelectric SrTiO3 by different approximations, J. Mod. Phys. 02 (2011) 934–943, https://doi.org/10.4236/jmp.2011.29111.

[5] W.J. Weber, R.C. Ewing, C.R.A. Catlow, T.D. de la Rubia, L.W. Hobbs, C. Kinoshita, H.j. Matzke, A.T. Motta, M. Nastasi, E.K.H. Salje, E.R. Vance, S.J. Zinkle, Radiation effects in crystalline ceramics for the immobilization of high-level nuclear waste and plutonium, J. Mater. Res. 13 (6) (1998) 1434–1484.

[6] W.J. Weber, A. Navrotsky, S. Stefanovsky, E.R. Vance, E. Vernaz, Materials science of high-level immobilization, MRS Bull. 34 (2009) 46–52, https://doi.org/ 10.1557/mrs2009.12.

[7] Ali, Z., Ahmad, I., Reshare, A.H.: Phys. B Condens. Matter 410, 1 (2012)

[8] Sahli, B., Bouafia, H., Abdellalli, A., Hiads, S., Akriche, A., Benkhettok, N., Rached, D.: J.Alloys Compd. 635, 163 (2015)

[9] Ali, Z., Ahmad, I. & Reshak, A. H. GGA+ U studies of the cubic perovskites BaMO3 (M= Pr, Th and U). Physica B: Condensed Matter 410, 217–221 (2013).

[10] Khandy, S. A. & Gupta, D. C. Structural, elastic and magneto-electronic properties of half-metallic BaNpO3 perovskite. Mater. Chem. Phys. 198, 380–385 (2017).

[11] Nabi, M., Bhat, T. M. & Gupta, D. C. Magneto-electronic, thermodynamic, and thermoelectric properties of 5 f-electron system BaBkO3. J. Superconduct. Novel Magn. 32, 1751–1759 (2019).

[12] Gautam, S., Ghosh, S., & Gupta, D. C. (2023). Understanding the computational insights of spin-polarised density functional theory into the newly half-metallic f electron-based actinide perovskites SrMO3 (M= Pa, Np, Cm, Bk). Scientific Reports, 13(1), 16882.

[13] Cañibano Crespo, M. E. (2004). Propriétés spectroscopiques de l'ion Yb3+ dans les familles d'oxydes de molybdates K5 Bi (MO4) 4, de grenats Y3 Al5 O12, Gd3 Ga5 O12, Lu3 Al5 O12 et de perovskites YAlO3: analyse de mécanismes d'extinction par concentration et évaluation de l'émission laser (Doctoral dissertation, Lyon 1).

[14] Martin, P. M., Le Naour, C., Charbonnel, M. C., Grandjean, S., Dacheux, N., & Moisy, P. (2021). La spéciation des actinides-Pierre angulaire de la chimie dans le cycle du combustible nucléaire. L'Actualité Chimique, (460-461).

[15] Runde,W.(2002). Geochemical interactions of actinides in the environment. Geochemistry of Soil Radionuclides, 59, 21-44.

[16] P. Zhao, J. Zhu, K. Yang, M. Li, G. Shao, H. Lu, J. He, Outstanding wear resistance of plasma sprayed high-entropy monoboride composite coating by inducing phase structural cooperative mechanism, Appl. Surf. Sci. 616 (2023), 156516, https:// doi.org/10.1016/j.apsusc.2023.156516.

[17] Abdullah M. Asiri, M.K. Shahzad, S. Hussain, Kai Zhu, S.B. Khan, K.A. Alamry, S. Y. Alfifi, H.M. Marwani, Analysis of XGaO3 (X = Ba and Cs) cubic based perovskite materials for photocatalytic water splitting applications: a DFT study, Heliyon 9 (3) (2023), e14112

[18] F. Bloch, Quantum mechanics of electrons in crystal lattices, Z. Phys 52 (1928) 555–600.

[19] D. Alfe, Ab initio molecular dynamics, a simple algorithm for charge extrapolation, Comput. Phys. Commun. 118 (1) (1999) 31–33.

[20] Gupta, D. C., & Ghosh, S. (2017). First-principal study of full Heusler alloys Co2VZ (Z= As, In). Journal of Magnetism and Magnetic Materials, 435, 107-116.